

Solution Structure of a Cisplatin-Induced DNA Interstrand Cross-Link

Huifang Huang,* Leiming Zhu,* Brian R. Reid, Gary P. Drobny,† Paul B. Hopkins†

The widely used antitumor drug *cis*-diamminedichloroplatinum(II) (*cis*-platin or *cis*-DDP) reacts with DNA, cross-linking two purine residues through the N7 atoms, which reside in the major groove in B-form DNA. The solution structure of the short duplex [d(CATAGCTAG)]₂ cross-linked at the GC:GC site was determined by nuclear magnetic resonance (NMR). The deoxyguanosine-bridging *cis*-diammineplatinum(II) lies in the minor groove, and the complementary deoxycytidines are extrahelical. The double helix is locally reversed to a left-handed form, and the helix is unwound and bent toward the minor groove. These findings were independently confirmed by results from a phase-sensitive gel electrophoresis bending assay. The NMR structure differs markedly from previously proposed models but accounts for the chemical reactivity, the unwinding, and the bending of *cis*-DDP interstrand cross-linked DNA and may be important in the formation and repair of these cross-links in chromatin.

Cisplatin is among the most widely used antitumor drugs (1). It is a bifunctional electrophile that forms covalent complexes in which cellular nucleophiles replace the chloride ligands (2). Cisplatin forms several types of lesions in DNA, including intrastrand and interstrand cross-links, with more of the former. Although considerable evidence indicates that the biological efficacy of the drug is the result of these DNA lesions (3), their relative efficacy remains unknown. The DNA cross-links bridge two purine residues, preferentially bridging the N7 sites at GG sequences in intrastrand cross-links (4) and GC sequences in interstrand cross-links (Fig. 1A) (5, 6). The DNA in these lesions must be structurally reorganized relative to canonical B-DNA because of the bond length and bond angle constraints imposed by the N7-Pt-N7 linkage.

Electrophoretic mobility measurements indicate that the interstrand cross-link bends the DNA (45°) (7, 8) and substantially unwinds it (80°) (8). The unwinding, in particular, defies a simple mechanical explanation based on an N7-Pt-N7 linkage in the major groove (6, 7), which appears more suited to overwind the duplex at the sequence GC. We report here a high-resolution solution structure of the *cis*-DDP interstrand cross-link in a short DNA duplex (9). An entirely unforeseen feature of the structure is that the *cis*-diammineplatinum(II) bridge resides in the minor, rather than the major, groove of the duplex.

The interstrand cross-linked 10-nucle-

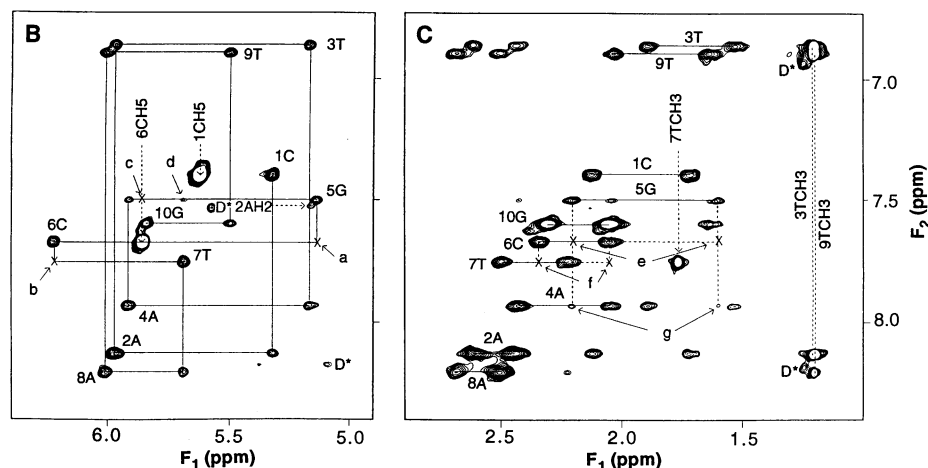
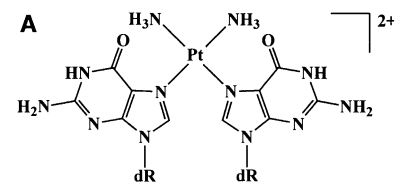
otide oligomer *cis*-diammineplatinum(II): [d(CATAGCTAG)]₂ was prepared by treatment of the corresponding DNA with aqueous *cis*-DDP (10). Through-bond DQF-COSY (11), through-space NOESY, and one-dimensional NOE proton connectivities were used to assign all nonexchangeable protons (except H5'/H5'') and all imino protons. Several irregularities in residues 4 through 7 (that is, the cross-linked base pairs and their immediate neighbors) indicated the presence of structural features

not normally present in B-DNA.

Several lines of evidence suggested that the cross-linked deoxyguanosine residues 5G and 5'G were not base paired to deoxycytidines 6'C and 6C, which were themselves not stacked in the duplex. For example, the imino proton 5GH1, readily assigned from its NOEs to the aromatic proton 4AH8 and the imino proton 7TH3, had a chemical shift of 9.6 ppm (12); this chemical shift is ~3 ppm upfield of that expected for a hydrogen-bonded GC pair and is more characteristic of an unpaired G (13). This conclusion was corroborated by the absence of NOEs sequentially linking 5G, 6C, and 7T and the unexpected presence of NOEs between 5G and 7T, which indicated their close proximity. Even at long mixing times, the NOEs 5GH1'-6CH6 and 6CH1'-7TH6 were undetectable (designated "a" and "b," respectively, in Fig. 1B). Similarly, the NOEs 5GH2'/H2''-6CH6 and 6CH2'/H2''-7TH6 were undetectable ("e" and "f" in Fig. 1C), as was the base-base NOE 5GH8-6CH5 ("c" in Fig. 1B). Instead, two unexpected NOEs were observed, indicating an unusually close proximity of 5G to 7T, namely 5GH8-7TH1' ("d" in Fig. 1B) and 5GH4'-7TH6 (12).

The weakness of the intrasidue NOEs 5GH2'/H2''-5GH8 indicated an unusual glycosidic angle for the cross-linked deoxyguanosines. Particularly striking, however, were NOE cross-peaks indicating the proximity of the 5GH2'/H2'' protons to the

Fig. 1. Covalent structure of *cis*-(NH₃)₂Pt:[d(CATAGCTAG)]₂ and ¹H NOESY (11) NMR spectra. **(A)** Covalent structure of a *cis*-DDP cross-link (upper), and sequence and cross-link location of DNA cross-linked by *cis*-DDP (lower). **(B)** The base-H1' region and **(C)** the base-H2'/H2'' region of the ¹H NOESY spectrum at a mixing time of 450 ms. The peaks designated D* are from impurities, and the letters a to d in (B) and e to g in (C) indicate NOEs discussed in the text. F₁ and F₂ designate the frequency in the first and second dimension, respectively.



H. Huang, L. Zhu, G. P. Drobny, P. B. Hopkins, Department of Chemistry, University of Washington, Seattle, WA 98195, USA.
B. R. Reid, Departments of Chemistry and Biochemistry, University of Washington, Seattle, WA 98195, USA.

*These authors contributed equally to this work.
†To whom correspondence should be addressed.

preceding base 4AH8 (Fig. 1C, "g") and to the preceding sugar 4AH1' (12), suggesting that 5G was not in an orientation typical of B-DNA.

The structure of the cross-linked DNA 10-nucleotide oligomer was derived as described previously (13). We used 630 distances derived from time-dependent NOE measurements, together with all distances implicit in the covalent structure, to generate a family of randomly embedded initial structures with distance geometry methods (14). These structures were further refined by molecular dynamics and energy minimization followed by iterative adjustment of the distances, guided by the experimental data with the program BIRDER (15), until

the differences between the simulated and experimental NOESY spectra were minimized to an *R* factor of less than 0.21. The 10 lowest energy structures were all highly converged based on all nonhydrogen atoms, with pairwise root mean square deviation values no greater than 0.55 Å (Fig. 2).

The refined structure (Fig. 2A) faithfully reflected the unusual features deduced from qualitative inspection of the NOEs, including the lack of a hydrogen-bonding partner for 5G and the extrahelicity of 6C (16). More surprising was the finding that the *cis*-diammineplatinum(II) was in the minor, rather than the major, groove, and there was an attendant, highly localized change of the double helix from a right-handed to a

left-handed, Z-DNA-like form (17) at 5G (Fig. 2B). The combination of the reversal of helix sense at 5G and the extrusion from the helix of 6C yielded a net unwinding of 87° relative to B-DNA over the three steps 4A to 7T. This structure neatly accounts for the conclusion, drawn from gel electrophoresis measurements, that this lesion unwinds DNA by ~80° (8); this unwinding cannot be rationalized by major groove models of the lesion. The helix axis is bent toward the minor groove at its effective center. The magnitude of this bend (20°) is smaller than that previously estimated from gel electrophoresis measurements (45°); the discrepancy may reflect inaccuracies in one or both methods.

Several features not present in B-DNA may stabilize this structure, including (i) cross-strand purine-purine stacking of 4A and 5'G, (ii) interaction of O4' of the sugar of 5G with the base of 7T (17), and (iii) electrostatic interaction of the pro-S oxyanions of the 5G and 5G' phosphate residues with the square planar platinum(II) atom (O-Pt distance, 3.2 Å), forming a pseudo-octahedral geometry around the metal atom (Fig. 2A) (18).

The NMR-derived structure, with the cross-link in the minor groove, the altered hydrogen bonding and base stacking, and the reversed sense of the double helix at the cross-link, differs substantially from previous models derived by molecular mechanics; these models place the cross-link in the major groove and substantially retain the hydrogen bonding and base stacking of B-DNA (6, 7). The NMR-derived structure explains the high chemical reactivity toward hydroxylamine of the unstacked cytosine bases at the cross-link (7), the low reactivity toward the minor groove-binding copper-phenanthroline reagent at the *cis*-diammineplatinum(II)-occupied minor groove (8), and most strikingly, the 80° unwinding caused by the expulsion of the deoxycytidine residues and the reversal of the helix sense at the cross-linked deoxyguanosine residues (8).

Electrophoretic measurements have shown that the *cis*-DDP interstrand cross-link bends the helix axis of DNA by ~45° (7, 8). The direction of the bend (that is, toward the minor or major groove) is unknown. An opportunity to distinguish between the NMR-derived and the theoretically derived structures was afforded by their predictions of bending in the opposite direction—the former toward the minor groove and the latter toward the major groove. We assigned the bend direction by reference to an A tract, which is bent by ~20° toward the minor groove (19), using electrophoretic retardation as a quantitative measure of the extent of planar curvature. The constructive (Fig. 3A, *cis*) and destructive (Fig. 3A,

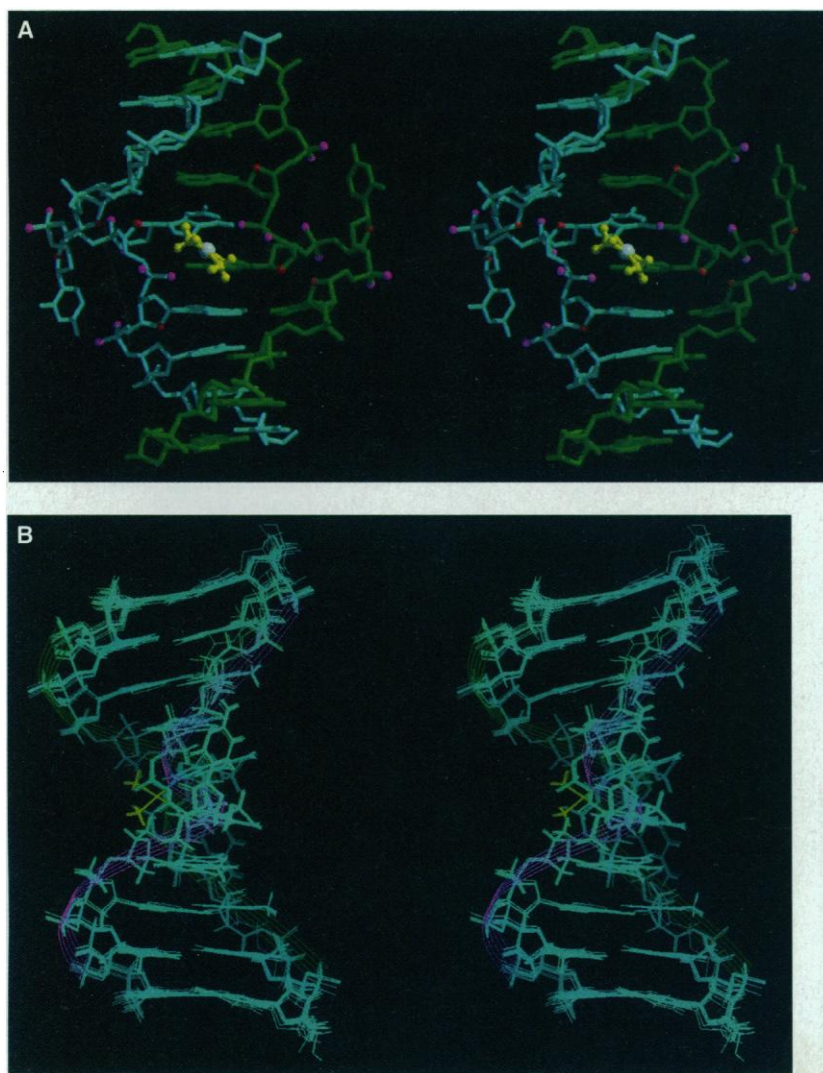


Fig. 2. Structure of *cis*-(NH₃)₂Pt:[d(CATAGCTATG)]₂. **(A)** Front stereoview (wide-eye) of one final structure with the lesion in the minor groove. Oxygen atoms in the sugar and phosphate backbone in residues 4 to 7 and 4' to 7' are highlighted to illustrate structural features not found in B-DNA, including (i) reversal of groove exposure of the base edges of 5G, (ii) inversion at 5G of the sugar geometry and helix sense reminiscent of Z-DNA, (iii) extrahelical residues 6C, (iv) cross-strand stacking of 4A and 5G', (v) interaction of 5GO4' with the base of 7T, and (vi) pseudo-octahedral ligand geometry at platinum(II). Platinum(II) atom, white; ammine groups, yellow; O4', red; and phosphate oxygens, purple. **(B)** Side stereoview (wide-eye) of the 10 lowest energy structures superimposed on one another, with the backbones highlighted by ribbons illustrating the helix sense reversal at the lesion.

trans) combinations of the *cis*-DDP bend (45°) and the A tract bend were expected to be readily distinguished.

Three *cis*-DDP-cross-linkable DNAs, P₃₃, P₃₄, and P₃₅, variable in length by a single base pair, were prepared in "native" and interstrand cross-linked forms (Fig. 3B). The 12 combinations of one of these six P DNAs admixed with an excess of either DNA A_{1,2} or A_{1,5}, which each contained an A tract in a different position, were enzymatically ligated to form multimers of the form A(PA)_n (20, 21). In the cross-linked multimers, the cross-links were separated by 33 to 35 base pairs (bp), corresponding to about three helical turns after the incorporation of the estimated 80° of unwinding at the lesion (8). The A tracts were located either "in phase," alternating one and two turns (A_{1,2}) from the cross-links, or "out of phase," 1.5 turns (A_{1,5}) from the cross-link.

The multimers lacking cross-links were of normal electrophoretic mobility, indicating that the A tracts were improperly phased to yield net planar curvature (Fig. 3, C and D). The cross-linked multimers were retarded relative to authentic size markers and thus bent. The retardation was maximal at a 33.8-bp separation of the cross-

links (Fig. 3D, inset), corresponding to ~90° of unwinding at the lesion (assuming a standard of 10.4 bp per helical turn) (8). The cross-linked multimers containing A_{1,2} were in all cases more retarded than those containing A_{1,5}, allowing assignment of the unit-turn separation of the A tract and cross-link as the *cis*-isomer (Fig. 3A). Hence, the effective bend of the helix axis at the center of the *cis*-DDP interstrand cross-link is in the same direction as that at the center of the A tract. Strong evidence indicates that the effective center of the A tract (19), and thus the *cis*-DDP interstrand cross-link, is bent toward the minor groove. The unwinding and direction of bending as revealed by the electrophoretic assay are thus consistent only with the NMR-derived structure (22).

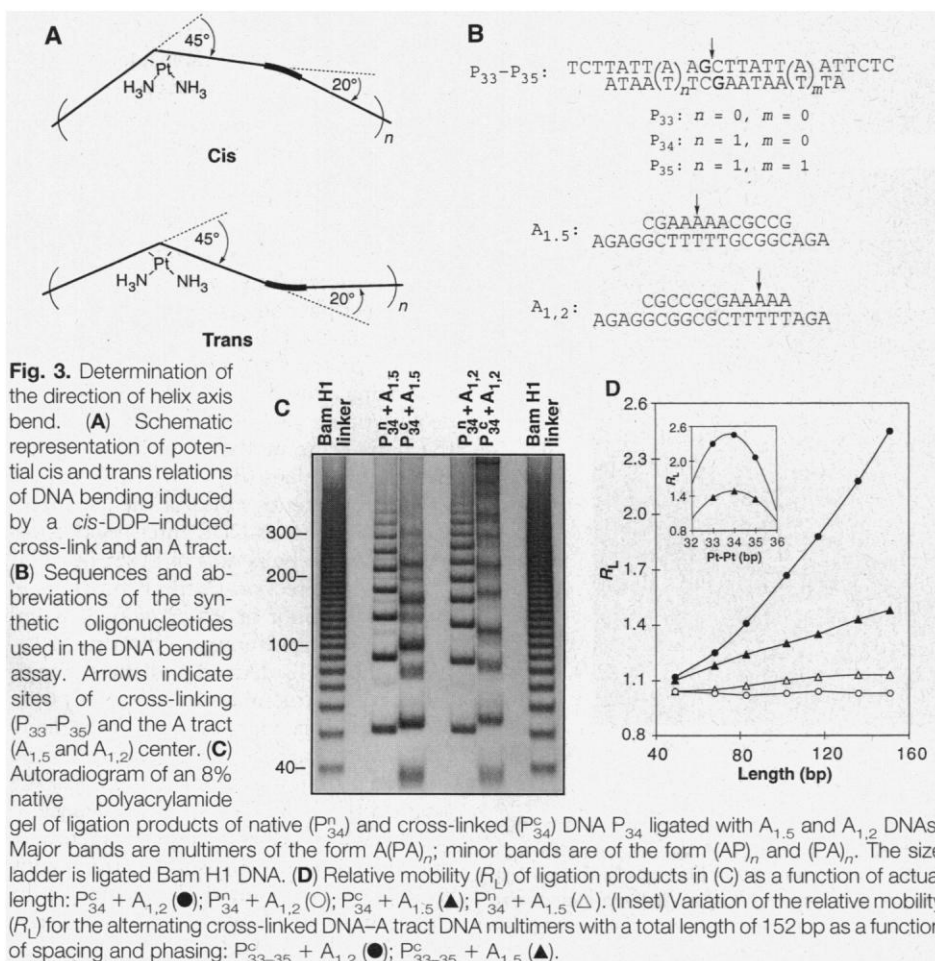
The structure we have described accounts for the chemical reactivity, the unwinding, and the bend direction of *cis*-DDP interstrand cross-linked DNA. The observation that the lesion in other flanking contexts is similarly bent and unwound, as well as cross-reactive with a common antibody that recognizes the cross-link (8), suggests that the general features of this structure are independent of the flanking nucleotide sequence. This structure raises mech-

anistic questions concerning the relative ordering of the bond-making and conformational reorganization steps and may be relevant to the slow rate at which monoadducts progress to cross-links (23). The structure may govern the locations at which this lesion is formed in chromatin as well as the identity of proteins that recognize or repair it. For example, the extrahelical residues may sequester or be altered by base-modifying or repair enzymes that require this structural feature (24). The structure of the more abundant, intrastrand cross-link appears to be very different (25), suggesting that the biological consequences of these two lesions will be distinct.

Note added in proof: Two papers on cisplatin-DNA adducts have appeared since this work was submitted. The solution structure (28) and the crystal structure (29) of intrastrand cross-linked DNAs both reveal the DNA to be bent toward the *cis*-diammineplatinum(II) group, which resides in the major groove. This is in contrast to our findings for the interstrand cross-linked DNA, and further indicates that this adduct is quite different structurally.

REFERENCES AND NOTES

- W. B. Pratt, R. W. Ruddon, W. D. Ensminger, J. Maybaum, *The Anticancer Drugs* (Oxford Univ. Press, New York, ed. 2, 1994), pp. 133-139.
- A. J. Tomson, *Recent Results Cancer Res.* **48**, 38 (1974).
- A. L. Pinto and S. J. Lippard, *Biochim. Biophys. Acta* **780**, 167 (1985); J. J. Roberts and F. Friedlos, *Pharmacol. Ther.* **34**, 215 (1987).
- A. Eastman, *Biochemistry* **24**, 5027 (1985).
- M. A. Lemaire, A. Schwartz, R. A. Rahmouni, M. Leng, *Proc. Natl. Acad. Sci. U.S.A.* **88**, 1982 (1991); P. B. Hopkins *et al.*, *Tetrahedron* **47**, 2475 (1991).
- H. Huang, J. Woo, S. C. Alley, P. B. Hopkins, *Bioorg. Med. Chem. Lett.* **3**, 659 (1995).
- M. Sip, A. Schwartz, F. Vovelle, M. Ptak, M. Leng, *Biochemistry* **31**, 2508 (1992).
- J.-M. Malinge, C. Pérez, M. Leng, *Nucleic Acids Res.* **22**, 3834 (1994).
- The structure of a bisplatinum-DNA complex has recently been reported [D. Yang *et al.*, *Nature Struct. Biol.* **2**, 577 (1995)].
- DNA was synthesized in three 10- μ mol runs as described (6) and used without further purification. Twenty-eight aliquots of 0.25 μ mol of the duplex [5'-d(CATAGCTATG)]₂ were treated sequentially with 420 μ l of aqueous *cis*-DDP (1.8 mM, 0.75 μ mol), 140 μ l of a solution of sodium perchlorate (400 mM) in 20 mM potassium phosphate buffer (pH 7.6), and 140 μ l of water and then allowed to stand at 25°C for 18 hours. The product was purified on 20 preparative gels as described (6), except that elution from the gel was shortened to 3 hours, followed by preparative high-performance liquid chromatography (HPLC) on a C18 column to yield 0.37 μ mol of cross-linked DNA (5% based on starting DNA).
- Abbreviations: DQF-COSY, double quantum filtered correlation spectroscopy; NOE, nuclear Overhauser enhancement; NOESY, nuclear Overhauser enhancement spectroscopy.
- H. Huang, L. Zhu, B. R. Reid, G. P. Drobny, P. B. Hopkins, data not shown.
- S.-H. Chou, L. Zhu, B. R. Reid, *J. Mol. Biol.* **244**, 259 (1994); L. Zhu, S.-H. Chou, B. R. Reid, *ibid.* **254**, 623 (1995).
- G. M. Crippen, *Distance Geometry and Conformational Calculations* (Research Studies Press, Wiley, New York, 1981).



15. L. Zhu and B. R. Reid, *J. Magn. Reson. Ser. B* **106**, 227 (1995).
16. The accuracy with which the position of the extrahe-
lical cytosine base is determined is questionable,
because it is in part defined by an electrostatic at-
traction between 6CH4 and a phosphate oxygen, for
which there is no experimental evidence.
17. A. H.-J. Wang *et al.*, *Science* **211**, 171 (1981).
18. A. H.-J. Wang, J. Nathans, G. A. van der Marel, J. H.
van Boom, A. Rich, *Nature* **276**, 471 (1978); K. J.
Barnham *et al.*, *Inorg. Chem.* **34**, 2826 (1995).
19. S. Zinkel and D. M. Crothers, *Nature* **328**, 178
(1987).
20. DNAs were synthesized and purified as described
(6) and (except for the upper strand of P₃₃-P₃₅)
exhaustively phosphorylated with T4 polynucleo-
tide kinase-adenosine triphosphate (ATP). Cross-
linked DNAs were prepared and purified (deleting
the HPLC step) as described (10). The upper
strands of P₃₃-P₃₅ were ³²P-labeled with T4
polynucleotide kinase-³²P-ATP then excess ATP
(26). A mixture of P and A in a 1:2 molar ratio was
exposed to T4 DNA ligase for 12 hours at 4°C, then
treated with eight additional molar equivalents of A
and fresh T4 DNA ligase and allowed to stand 24
hours at 4°C. Samples were analyzed by polyacryl-
amide gel electrophoresis (PAGE) as described
(27).
21. This experiment is analogous to that reported for the
cis-DDP intrastrand cross-link [J. A. Rice, D. M.
Crothers, A. L. Pinto, S. J. Lippard, *Proc. Natl. Acad.
Sci. U.S.A.* **85**, 4158 (1988)].
22. The empirical relation of Koo and Crothers [H.-S.
Koo and D. M. Crothers, *Proc. Natl. Acad. Sci.
U.S.A.* **85**, 1763 (1988)], which converts relative
length (R_i) to a bend angle, afforded values of 55°
and 31° per three turns, respectively, for the *cis*-(P₃₄
-A_{1,2}) and *trans*-(P₃₄-A_{1,5}) isomers (at 152 bp), in
relatively good agreement with the expected values
of 65° and 25°.
23. D. Payet, F. Gaucheron, M. Sip, M. Leng, *Nucleic
Acids Res.* **21**, 5846 (1993).
24. S. Klimasauskas, S. Kumar, R. J. Roberts, X. Cheng,
Cell **76**, 357 (1994); R. Savva, K. McAuley-Hecht, T.
Brown, L. Pearl, *Nature* **373**, 487 (1995); C. D. Mollet
et al., *Cell* **80**, 869 (1995); H.-W. Park, S.-T. Kim, A.
Sancar, J. Deisenhofer, *Science* **268**, 1866 (1995);
K. M. Reinisch, L. Chen, G. L. Verdine, W. N. Lips-
comb, *Cell* **82**, 143 (1995).
25. F. Herman *et al.*, *Eur. J. Biochem.* **194**, 119 (1990).
26. S. M. Rink and P. B. Hopkins, *Biochemistry* **34**, 1439
(1995).
27. H.-S. Koo, H.-M. Wu, D. M. Crothers, *Nature* **320**,
501 (1986).
28. D. Yang, S. G. E. van Boom, J. Reedijk, J. H. van
Boom, A. H.-J. Wang, *Biochemistry* **34**, 12912
(1995).
29. P. M. Takahara, A. C. Rosenzweig, C. A. Frederick,
S. J. Lippard, *Nature* **377**, 649 (1995).
30. Supported by NIH grants GM32681 (G.P.D., P.B.H.,
and B.R.R.) and GM45804 (P.B.H.) and by research
contract 224016 under Master Agreement 206001-
A-L2 from Battelle Pacific Northwest Laboratory
(G.P.D.). We thank V. C. Yee and R. Stenkamp for
assistance in the preparation of Fig. 2 and W. Mc-
Callister for technical assistance.

9 August 1995; accepted 30 October 1995

Role of NK1.1⁺ T Cells in a T_H2 Response and in Immunoglobulin E Production

Tomohiro Yoshimoto,* Albert Bendelac, Cynthia Watson,
Jane Hu-Li, William E. Paul†

Immune responses dominated by interleukin-4 (IL-4)-producing T helper type 2 (T_H2) cells or by interferon γ (IFN- γ)-producing T helper type 1 (T_H1) cells express distinctive protection against infection with different pathogens. Interleukin-4 promotes the differentiation of naïve CD4⁺ T cells into IL-4 producers and suppresses their development into IFN- γ producers. CD1-specific splenic CD4⁺NK1.1⁺ T cells, a numerically minor population, produced IL-4 promptly on in vivo stimulation. This T cell population was essential for the induction of IL-4-producing cells and for switching to immunoglobulin E, an IL-4-dependent event, in response to injection of antibodies to immunoglobulin D.

Interleukin-4 is a major determinant of the differentiation of naïve T cells into IL-4-producing cells and has the capacity to suppress their differentiation into IFN- γ -producing cells (1). A potential source of IL-4 that could affect the priming of naïve CD4⁺ T cells is a set of CD4⁺NK1.1⁺ splenic T cells (2). These cells produced IL-4 within 30 to 90 min of in vivo challenge with antibody to CD3 or with staphylococcal enterotoxin B. They appear to be related to a population of thymic NK1.1⁺ T cells that are also prompt cytokine producers (3–9). NK1.1⁺ thymocytes are known to express a limited set of $\alpha\beta$ T cell receptors (TCR $\alpha\beta$) specific for the major histocompatibility complex (MHC) class I-like molecule CD1 (3, 4, 7–10). Thymic NK1.1⁺ T cells were markedly diminished

in number in β_2 -microglobulin knockout (β_2 M^{-/-}) mice (3, 11). This is in keeping with the association of β_2 M with CD1 (12).

Splenic CD4⁺NK1.1⁺ T cells were also markedly diminished in β_2 M^{-/-} mice (Fig. 1A), constituting only 0.1% of spleen cells in contrast to a frequency of 1.0% in C57BL/6 mice (13). In CD8^{-/-} C57BL/6 congenic mice, the frequency of CD4⁺NK1.1⁺ T cells was similar to that in C57BL/6 mice. MHC class II^{-/-} ($A\beta$ ^{-/-}) mice expressed almost the same number of CD4⁺NK1.1⁺ splenic T cells as were expressed by C57BL/6 mice, although CD4⁺ T cells constituted only 4 to 5% of their spleen cells. CD4^{-/-} mice did not express any CD4⁺NK1.1⁺ cells but did express NK1.1⁺ T cells, as determined by staining with antibodies to CD3 and NK1.1 (14).

As anticipated from their deficiency of CD4⁺NK1.1⁺ cells, β_2 M^{-/-} mice made minimal or no IL-4 90 min after injection of antibody specific for CD3, whereas C57BL/6, $A\beta$ ^{-/-}, CD8^{-/-}, and CD4^{-/-} mice all produced IL-4 (Fig. 1B). In contrast, IL-2 and IFN- γ were produced in response to antibody to CD3 by spleen cells from C57BL/6 mice and from each strain of the knockout mice,

including β_2 M^{-/-} mice. This indicates that CD4⁺NK1.1⁺ T cells are not uniquely responsible for the production of IL-2 and IFN- γ . Antibody to CD3 also failed to stimulate β_2 M^{-/-} mice to produce messenger RNA (mRNA) for IL-13, a cytokine closely related to IL-4, whereas each of the other strains produced IL-13 mRNA (14).

If the IL-4 that is rapidly produced by CD4⁺NK1.1⁺ T cells is important in the commitment to the T_H2 pathway of T cell development, β_2 M^{-/-} mice would be deficient in immunoglobulin E (IgE) production, as IL-4, a T_H2 product, is the major determinant of IgE production in mice (15, 16). Immunoglobulin E is markedly induced in several mouse strains by injection of the polyclonal stimulant goat antibody to mouse IgD (anti-IgD) (17). Treatment with antibody to IL-4 (anti-IL-4) completely inhibits such production of IgE (15). We have used this model to examine the IgE-producing potential of β_2 M^{-/-} mice. Normal C57BL/6 mice, $A\beta$ ^{-/-} mice, and CD8^{-/-} mice each developed substantial and comparable IgE responses to anti-IgD (Fig. 1C). In contrast, β_2 M^{-/-} mice made minimal or no IgE in response to an in vivo challenge with anti-IgD. CD4^{-/-} mice also made diminished amounts of IgE in response to anti-IgD, although these mice made normal amounts of IL-4 90 min after injection with antibody to CD3.

Not only did β_2 M^{-/-} mice fail to produce IgE in response to injection of anti-IgD, but their spleen cells failed to secrete IL-4 spontaneously 5 days after injection of anti-IgD and showed only modest IL-4 production when stimulated in vitro with anti-IgD (Fig. 2). In contrast, C57BL/6 spleen cells produced IL-4 5 days after injection with anti-IgD, and that production was enhanced by culture with anti-IgD, presumably because of the recognition of anti-IgD peptides bound to MHC class II molecules. β_2 M^{-/-} mice can be primed in vivo to

T. Yoshimoto, C. Watson, J. Hu-Li, W. E. Paul, Laboratory of Immunology, National Institute of Allergy and Infectious Diseases, National Institutes of Health, Bethesda, MD 20892, USA.

A. Bendelac, Department of Molecular Biology, Princeton University, Princeton, NJ 08544, USA.

*Present address: Department of Immunology and Medical Zoology, Hyogo College of Medicine, 1-1, Mukogawa, Nishinomiya 663, Japan.

†To whom correspondence should be addressed.